RSC Advances

ROYAL SOCIETY OF CHEMISTRY

www.rsc.org/advances

RSC Advances

ARTICLE

Anthanthrene dye-sensitized solar cells: influence of the number of anchoring groups and substitution motif

Received 00th January 20xx,
Accepted 00th January 20xx

DOI: 10.1039/x0xx00000x

www.rsc.org/

Yan Geng,[a] Chenyi Yi,[b] Martin Peter Bircher,[c] Silvio Decurtins,[a] Michele Cascella,[d] Michael Grätzel,[b] and Shi-Xia Liu*[a]

Four new dye molecules comprising an anthanthrene core, thiophene-cyanoacrylic acid electron acceptor and triphenylamine (TPA) electron donor units were prepared. Thereby, the substitution pattern at the anthanthrene core has been varied systematically. The molecules were fully characterized using optical spectroscopy and cyclic voltammetry, and their electronic structures and excitation energies were calculated by DFT and TDDFT methods. The photovoltaic properties of dye-sensitized solar cells based on these molecules were investigated. In comparison to symmetric dyes, the introduction of the organic donor TPA in asymmetric dyes leads to a remarkable improvement of the solar energy conversion efficiencies due to higher V_{oc} and J_{sc} values of devices, giving rise to the best overall efficiency of 5.27%.

Introduction

Anthanthrene, the compact polycyclic aromatic hydrocarbon (PAH) dibenzo[def,mno]chrysene, its angular counterpart, dibenzo[*b*,def]chrysene, as well as their soluble derivatives represent promising building blocks for many applications in the field of materials science.[1] Importantly, what sets these prototypical nonlinear PAHs apart from linearly fused acenes, such as anthracene and pentacene, is the enhanced stability towards degradative chemical reactions and photooxidation.[2] Within the field of organic light-emitting diodes (OLEDs), the photophysical properties of anthanthrene derivatives have been investigated for their tunable blue emission characteristics.[3] More recently, a study of noncoherent photon upconversion systems with improved energy conversion efficiencies found that anthanthrene functions as an efficient triplet acceptor and upconverter in combination with C60, even so the latter is a poor visible photon absorber.[4] The anthanthrene moiety has also been used as a component for the construction of belt-persistent tubular cycloarylenes, where π-contact motifs assist the formation of interesting solid-state columnar assemblies.[5] Not surprisingly, anthanthrene derivatives have been probed as semiconductors for organic field-effect transistors and as active components for organic bulk heterojunction (BHJ) solar cells.[6,7] Due to the large π-conjugated core structure, strong π-π interactions can lead to favorable packing motifs, beneficial for large orbital overlap. As a case in point, Morin and co-workers recently reported power conversion efficiencies up to 2.4% for organic BHJ solar cells with a few cruciform anthanthrene derivatives.[7]

We are particularly interested in this class of polycyclic compounds because it has recently been demonstrated by the group of Morin[2a,8] that the 4,10-dibromoanthanthrone precursor offers two axes of functionalization: the ketones at the 6,12-positions (short-axis) and the bromines at the 4,10-positions (long-axis). These studies have led the authors to suggest that there is a more effective π-conjugation through the aromatic core along the 6,12-axis than along the 4,10-axis. In a recent study in the context of molecular electronics, we investigated the connectivity-driven electrical conductance of two anthanthrene derivatives that were anchored in a mechanically controllable break junction separately along the short-axis and long-axis. Thereby, the short-axis contacted anthanthrene showed about an 80 times higher conductance than the long-axis contacted one; these findings were consistently corroborated by theory.[9] Furthermore, despite the fact that anthanthrene derivatives are used as dye materials, anthanthrene-based sensitizers for application in dye-sensitized solar cells (DSSCs) have not been explored yet. Therefore, we envisaged to use the different substitution options offered by the core moiety of 4,10-dibromoanthanthrone for an appropriate functionalization. Taking an anchoring group like cyanoacrylic acid linked to a thiophene unit, which simultaneously acts as an electron acceptor,[10] renders at the same time a molecular electron donor (D) – electron acceptor (A) system. As it is well

[a] Department of Chemistry and Biochemistry, University of Bern, Freiestrasse 3, CH-3012 Bern, Switzerland. E-mail: liu@dcb.unibe.ch.
[b] Laboratory of Photonics and Interfaces, Institute of Chemical Science and Engineering, École Polytechnique, Fédérale de Lausanne (EPFL), Station 6, CH-1050 Lausanne, Switzerland.
[c] Laboratory of Computational Chemistry and Biochemistry, EPFL SB ISIC LCBC, BCH 4110 (Batochime UNIL), Av. F.-A. Forel 2, CH-1050 Lausanne, Switzerland.
[d] Department of Chemistry and Centre for Theoretical and Computational Chemistry (CTCC), University of Oslo, PO Box 1033 Blindern, N-0315 Oslo, Norway.
Electronic Supplementary Information (ESI) available: optical absorption spectra of four dyes absorbed on TiO_2 films and the detailed information on DFT calculations. See DOI: 10.1039/x0xx00000x

established, molecular D – A assemblies give rise to photoinduced intramolecular charge-transfer (ICT) transitions,[11] also exhibiting a beneficial directionality of charge transfer towards the anchoring acceptor group.[12] This ICT effect could additionally be enhanced by further functionalization of the core unit with a triphenylamine donor. Herein, we present the synthesis, electronic properties and DSSC performances of four new anthanthrene based dye molecules (Chart 1). The aim of this study is to investigate the influence of the number of cyanoacrylic acid anchoring groups as well as substitution through the anthanthrene core along the 6,12-axis and the 4,10-axis on the overall efficiencies of solar cells.

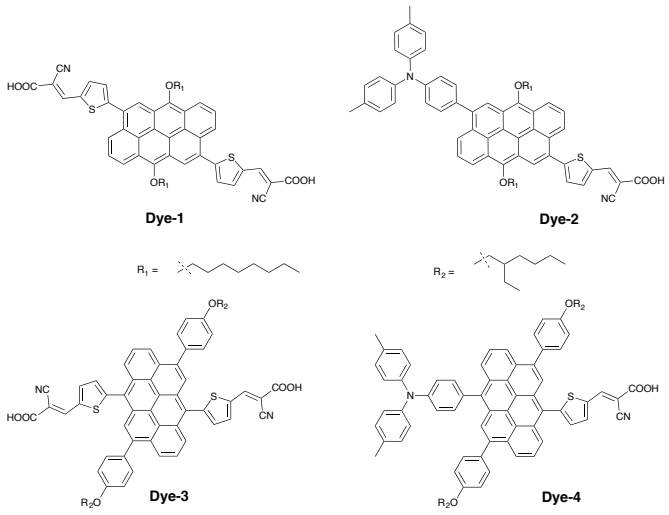

Chart 1 Chemical structures of four target dyes.

Results and discussion

Synthesis and Characterization

The synthetic routes to the anthanthrene photosensitizers are shown in Schemes 1 and 2. In the first synthetic step, the reduction-alkylation reaction was performed to improve the solubility of the 4,10-substituted anthanthrene-based **Dye-1** and **Dye-2** by introducing alkyl group at 6,12-positions.[8a] Both dyes are synthesized *via* a Knoevenagel reaction of the corresponding aldehyde precursor **2** or **5** with cyanoacetic acid. The former was readily obtained either from compound **1** in 46% yield or from the compound **4** in 77% yield by Suzuki reaction with an excess of 5-carboxythiophene-2-boronic acid under microwave condition. The asymmetric **Dye-2** was accomplished by sequentially applying a Suzuki reaction. First, a triphenylamine (TPA) donor commonly used for molecular sensitizers, was embedded on the anthanthrene backbone by reacting one equivalent of triphenylamine boronic ester with compound **1** to yield compound **4** in 49% yield.

Similarly, for the preparation of **Dye-3** and **Dye-4** illustrated in Scheme 2, it is also important to introduce solubilizing groups to the anthanthrene core prior to functionalization with cyanoacetic acid and TPA groups. A standard Suzuki reaction between 4-(2-ethylhexyloxy)phenyl-4,4,5,5-tetramethyl-1,3,2-dioxaborolane and 4,10-dibromoanthanthrone was performed to afford **6** in 70% yield. The subsequent BH_3 reduction led to the formation of compound **7** in 21% yield. The successful bromination of **7** in the presence of Br_2 allowed us to further modify the anthanthrene backbone at the 6-position and 12-position. The key precursor **8** was obtained in 86% yield. Following the same synthetic strategy as for **Dye-1** and **Dye-2**, the symmetric **Dye-3** and the asymmetric **Dye-4** were synthesized in good yields starting from **8**. All precursor and target compounds have been fully characterized. Their NMR spectroscopic and high resolution mass spectrometric data are consistent with their proposed structures and elemental compositions.

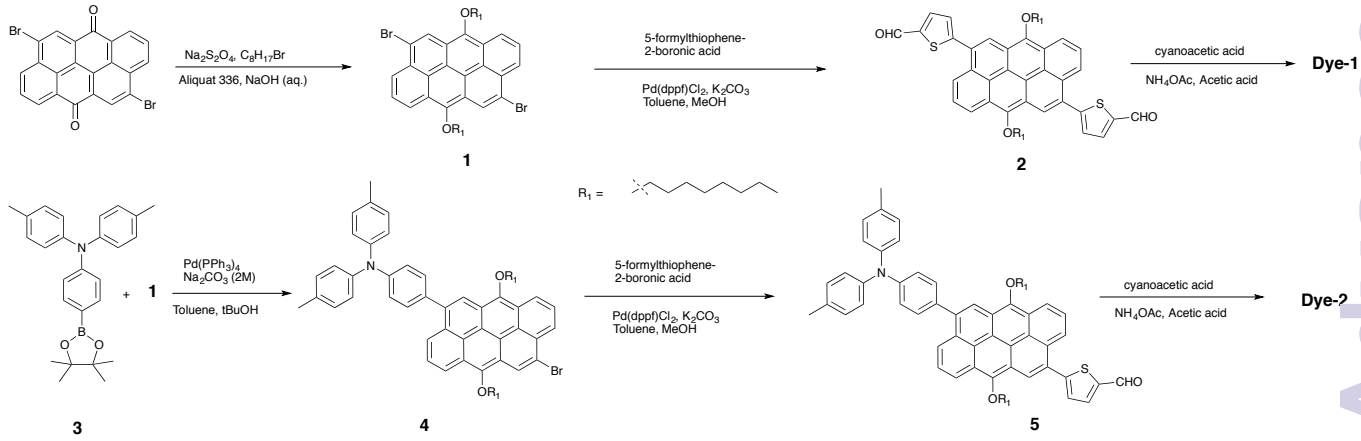

Scheme 1 Synthesis of **Dye-1** and **Dye-2**.

Photophysical Properties

The optical absorption and emission spectra of **Dye-1** to **Dye-4** are depicted in Figure 1. In the UV spectral region, below 400 nm, all four dyes show strong absorptions of varying appearances. In the visible spectral region, they all exhibit their intense lowest energy absorption band between 460 and 465 nm. The characteristics of selected absorption bands hence the orbital nature of their corresponding electronic transitions, will be discussed below on the basis of theoretical

calculations. On closer inspection, it is found that some spectral features depend on substitution motifs through either the 6,12-axis or 4,10-axis. For instance, **Dye-1** and **Dye-2** display intense broad absorption bands over the whole spectral range from 350 nm to 500 nm, whereas **Dye-3** and **Dye-4** show only little intensity around 400 nm; however there is no simple interpretation for it (*vide infra*)

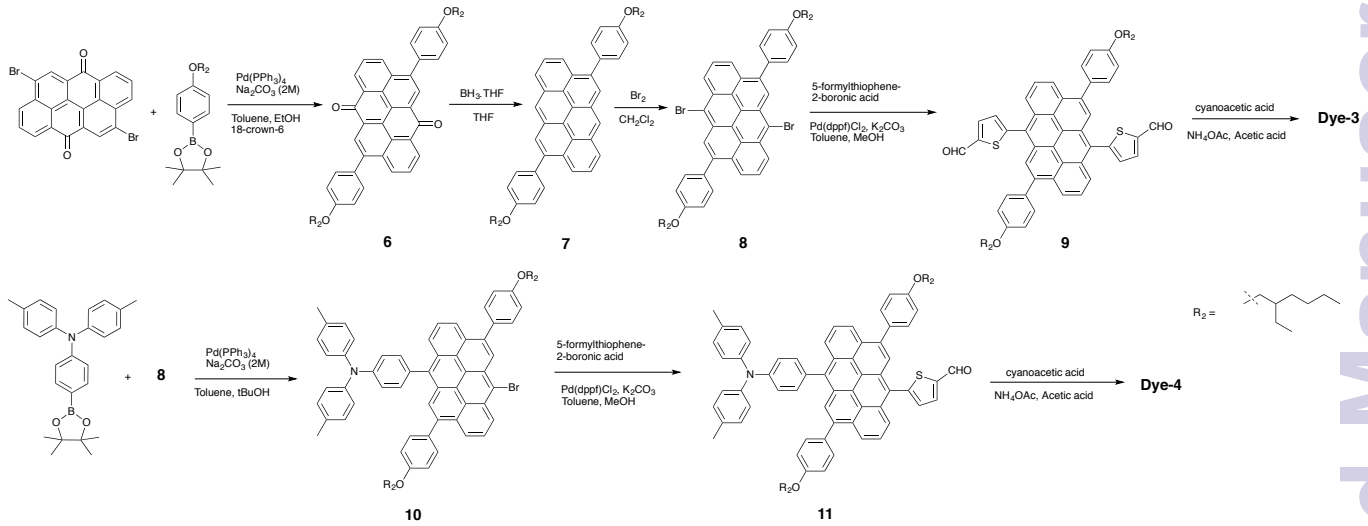

Scheme 2 Synthesis of **Dye-3** and **Dye-4**.

All four dyes are only weakly emissive. Notably, there are distinctly larger Stokes shifts observed for the symmetric **Dye-1** (5900 cm^{-1}) and **Dye-3** (5100 cm^{-1}) than for the asymmetric **Dye-2** (3300 cm^{-1}) and **Dye-4** (3400 cm^{-1}) (Table 1), revealing a larger displacement on the nuclear coordinates for the S_0/S_1 states of the former due to the extension of the π-conjugation of the anthanthrene unit compared to those of the latter molecules.

In addition, the absorption spectra of **Dye-1** to **Dye-4** adsorbed on a TiO_2 film (see Figure S1) show that the lowest-energy absorption bands, compared to those in THF, are substantially red-shifted.

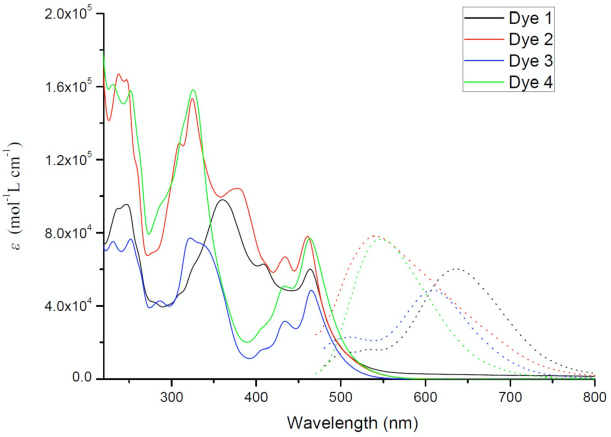

Fig. 1 UV-vis absorption (solid line) and fluorescence (dash line) spectra of **Dye-1** to **Dye-4** in THF solutions; λ_{ex} = 465 nm.

DFT calculations

To assign the orbital nature of the electronic transitions in the four compounds **Dye-1** to **Dye-4**, theoretical calculations were performed at the DFT/M06 level for geometry optimization and at the TDDFT/M06-2X level for the electronic excitations. The ground-state geometries of all four dyes were optimized with no symmetry constraints. The anthanthrene cores are virtually planar and the dihedral angles with the pendant thiophene rings range from 51° to 85°. Figure 2 shows the important frontier molecular orbitals (MOs) together with their calculated energies. The symmetric **Dye-1** and **Dye-3** exhibit a localization of their π-type HOMOs on the anthanthrene core whereas the LUMO and LUMO+1 largely represent the in- and out-of-phase linear combinations of the π-type orbitals located on the attached thiophene-cyanoacrylic acid substituents; only for the LUMO of **Dye-1** there is also substantial electron-density localization on the perimeter of the central unit. For the asymmetric **Dye-2** and **Dye-4**, their π-type HOMOs are as well localized on the central cores and their π-type LUMOs are spread over the whole thiophene-cyanoacrylic acid substituents. The LUMO+1 is for both asymmetric compounds again located on the anthanthrene core. Now, the triphenylamine moieties, in agreement with their electron donating character, show electron density localization within the corresponding HOMO-1. It is noteworthy that the larger dihedral angles (calculated values range from 84° to 85°) between the anthanthrene core and the thiophene rings in **Dye-3** and **Dye-4**, caused by the steric hindrance from phenyl rings at the 4,10-positions, to some extent limit the orbital delocalization beyond the anthanthrene. This result may account for the aforementioned experimental fact that **Dye-1** and **Dye-2** show intense broad absorption bands in the whole range from 350 nm to 500 nm in contrast to **Dye-3** and **Dye-4**.

The optical absorption spectra can be well analysed on the basis of the calculated vertical electronic transitions. Figures S2 to S5 display the optical spectra together with the

corresponding stick plots while Tables S1 to S4 give the corresponding major orbital contributions for the electronically excited states. For the symmetric **Dye-1** and **Dye-3**, the energetically lowest electronic transitions with high intensities are the $S_0 \rightarrow S_2$ and $S_0 \rightarrow S_1$ excitations which are dominated by a one-electron HOMO → LUMO and HOMO → LUMO+1 promotions, respectively. Thus, electron density is moved from the central anthanthrene core to the substituents on the 4,10-positions and 6,12-positions, respectively. In both cases, the oscillator strengths conform well to the experimentally determined extinction coefficients and the calculated energies agree reasonably well with the lowest energy absorption band. The same holds for the higher energy absorption bands. For the asymmetric **Dye-2** and **Dye-4**, the $S_0 \rightarrow S_1$ and $S_0 \rightarrow S_2$ excitations are essentially mixtures of HOMO → LUMO and HOMO → LUMO+1 transitions; the details depend on the chosen functional (see computational modelling). Importantly, they reflect charge transfer from the central core to the thiophene bearing unit as well as anthanthrene based π→π* characteristics. Again, the calculated energies and oscillator strengths compare fairly well with the lowest energy absorption bands of each compound; the same holds for the higher energy region.

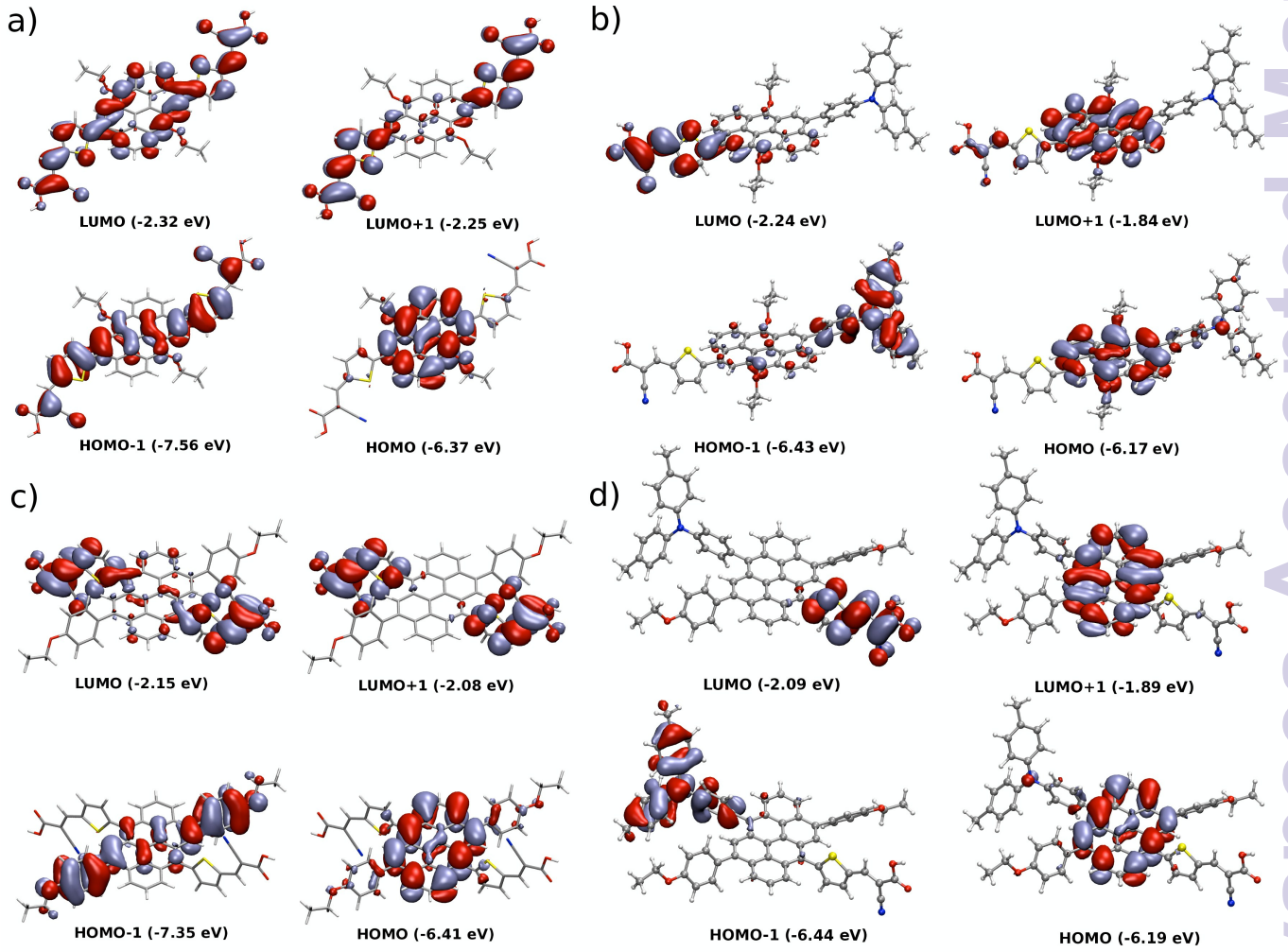

Fig. 2 Selected frontier molecular orbitals of **Dye-1** (a), **Dye-2** (b), **Dye-3** (c) and **Dye-4** (d).

Electrochemical Properties

The electrochemical properties of the four dyes in CH_2Cl_2 were investigated by cyclic voltammetry (CV) (Figure 3). Both symmetric **Dye-1** and **Dye-3** with two cyanoacrylic acid anchoring groups exhibit only one reversible oxidation wave nearly at the same potential, typical for the oxidation of the anthanthrene core. In contrast, **Dye-2** and **Dye-4** undergo two reversible oxidation processes due to the sequential oxidation of the anthanthrene and TPA units.

The combination of the optical and CV data allows the determination of the HOMO and LUMO energy levels (Table 1). By replacing one thiophene-cyanoacrylic acid electron accepting group by the TPA electron donating unit, makes clearly a difference, as seen by the increasing LUMO values within the pairs of the long-axis or short-axis substituted dyes. Analogously, the HOMOs get destabilized as well by replacing

one acceptor with a donor substituent. However, within the energy range of the frontier MOs, there is no pronounced effect of the 4,10- *vs* 6,12-substitution motif. The same trends were also seen in the computational study.

Notably, the four dyes have an appropriate LUMO level which is sufficiently more negative than the conduction band of TiO_2, indicating that photo-excited electrons can be effectively injected into the conduction band of TiO_2.[13] Also all of them have a relatively low-lying HOMO energy level in a range of -5.06 eV to -5.30 eV, which is lower than the energy level of the iodine/iodide redox mediator, therefore ensuring efficient regeneration of the oxidized dye and also good air stability in DSSC devices.[14]

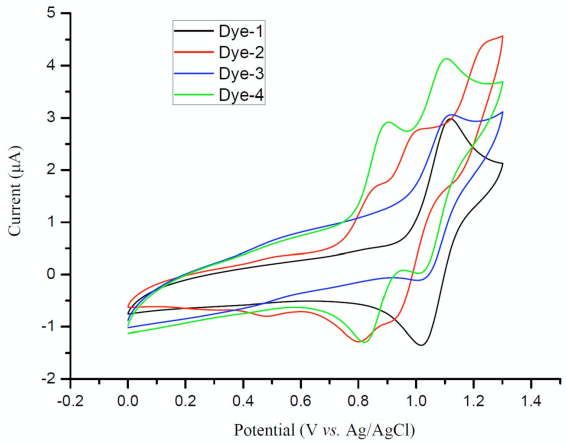

Fig. 3 Cyclic voltammograms of **Dye-1** to **Dye-4** in CH_2Cl_2 (0.1 M Bu_4NPF_6; Pt-disk working electrode; scan rate 100 mVs^{-1}).

Table 1 Lowest energy absorption and emission maxima, A_{max} and E_{max} respectively, extinction coefficient ε, onset oxidation potentials E, optical band gaps E_g^{opt} and calculated HOMO and LUMO energy levels of **Dye-1** to **Dye-4** in THF.

	A_{max} (nm, ε (10^5 M^{-1} cm^{-1}))	E_{max} (nm)	$E_{g,opt}$ [a] (eV)	E [b] (V)	E_{HOMO} [c] (eV)	E_{LUMO} [d] (eV)
Dye-1	464 (0.60)	637	2.38	0.49	-5.29	-2.91
Dye-2	461 (0.78)	539	2.56	0.26	-5.06	-2.50
Dye-3	463 (0.49)	608	2.44	0.50	-5.30	-2.86
Dye-4	464 (0.77)	548	2.49	0.30	-5.10	-2.61

[a] Optical band gap is estimated from the cross point of absorption and emission spectra. [b] The first oxidation potential of Fc^+/Fc against Ag/AgCl was recorded in CH_2Cl_2-Bu_4NPF_6 (0.1 M) solution to be 0.49 V, therefore the onset oxidation potentials are referred to Fc^+/Fc by subtracting 0.49 V from Ag/AgCl values. [c] HOMO level is calculated from the onset of the first oxidation potential in cyclic voltammetry according to the equation $E_{HOMO} = [-e(E_{onset} + 4.8)]$ eV, where 4.8 eV is the energy level of ferrocene below the vacuum level. [d] LUMO level is estimated according to the equation $E_{LUMO} = [E_{g,opt} + E_{HOMO}]$ eV.

Photovoltaic Properties of DSSCs Based on Dye-1 to Dye-4

DSSCs were fabricated using the synthesized dyes according to the methods described in the Experimental section. The detailed photovoltaic parameters, including short-circuit photocurrent density (J_{sc}), open-circuit voltage (V_{oc}), fill factor (*FF*), and conversion efficiency (η), are listed in Table 2. The efficiency of the DSSCs based on the synthesized dyes increases gradually in the order of **Dye-3** < **Dye-1** < **Dye-4** < **Dye-2**. In comparison to symmetric dyes (**Dye-1** and **Dye-3**) that show a strong aggregation propensity on the TiO_2 surface, the introduction of the organic donor TPA in asymmetric dyes (**Dye-2** and **Dye-4**) leads to a remarkable improvement of the solar energy conversion efficiencies due to higher dye loading in the latter cases. The higher V_{oc} values of devices based on **Dye-3** and **Dye-4** can be accounted for the fact that the presence of the appended phenyl units at 4,10-positions of the anthanthrene core prevents the leakage of photo-excited electrons from TiO_2 to the redox mediator / the oxidized dye, thus the recombination processes can be effectively suppressed. In contrast, devices based on **Dye-1** and **Dye-2** show the higher J_{sc} values, again because of the steric hindrance effect of the appended phenyl units at 4,10-positions of the anthanthrene core which renders the conjugation through the 6,12-axis much less effective, once again corroborating the observation that intense absorption bands spread across a much broader visible spectral range for **Dye-1** and **Dye-2** than for **Dye-3** and **Dye-4**. Taking all these structural parameters into consideration, **Dye-4** based DSSC devices show the highest V_{oc} while **Dye-2** based devices display the highest J_{sc}, giving rise to the best overall efficiency of 5.27%. Moreover, despite of their symmetric and asymmetric structural patterns, 4,10-substituted dyes (**Dye-1** and **Dye-2**) exhibit a better efficiency than the corresponding 6,12-substituted ones (**Dye-3** and **Dye-4**).

Table 2 Photovoltaic performances of DSSCs based on **Dye-1** to **Dye-4**.

	J_{sc}(mA cm^{-2})	V_{OC} (mV)	*FF*	η (%)
Dye-1	8.18	606	0.75	3.73
Dye-2	10.40	690	0.73	5.27
Dye-3	6.54	658	0.76	3.28
Dye-4	8.19	738	0.76	4.58

Conclusions

In summary, we have presented a series of a new type of photosensitizers which are based on the polycyclic anthanthrene molecule, namely **Dye-1** to **Dye-4**, either with one or two cyanoacrylic acid anchoring groups linked through a thiophene unit to the 6,12-positions or the 4,10-positions of the anthanthrene core. For the first time, anthanthrene-based DSSCs are described, showing PCEs of up to 5.27%. Moreover, the electronic structures and excitations of all four dyes were investigated by quantum mechanical calculations that fully support the experimental results. A detailed and systematic study on the anthanthrene dyes through the structural modification in order to extend their spectral response to the long wavelength region and therefore enhance the DSSC performance is currently underway.

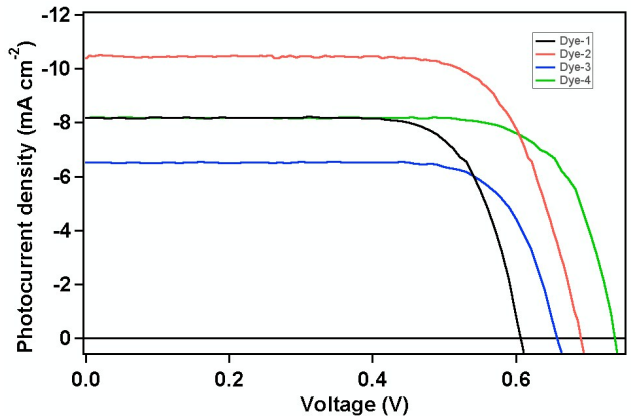

Fig. 4 Photovoltaic performance of **Dye-1** to **Dye-4**. (a) Photocurrent action spectra showing the incident photon-to-current conversion efficiency as a function of excitation wavelength. (b) Photocurrent density (*J*) as a function of voltage (*V*) measured under standard air mass 1.5 and simulated sunlight at 1000 W/m^2 intensity.

Experimental

General Experimental Procedures

Air and/or water-sensitive reactions were conducted under argon or nitrogen in dry, freshly distilled solvents. ^{1}H and ^{13}C NMR spectra were recorded on a Bruker Avance 300 spectrometer (300 MHz for ^{1}H and 75 Hz for ^{13}C). Chemical shifts are reported in parts per million (ppm) and are referenced to the residual solvent peak (chloroform, ^{1}H = 7.26 ppm, ^{13}C = 77.16 ppm; DMSO, ^{1}H = 2.5 ppm, ^{13}C = 39.52 ppm; CD_2Cl_2, ^{1}H = 5.32 ppm, ^{13}C = 54.0 ppm; THF, ^{1}H = 3.58 ppm, ^{13}C = 67.57 ppm). Coupling constants (*J*) are given in hertz (Hz) and are quoted to the nearest 0.5 Hz. Peak multiplicities are described in the following way: s, singlet; d, doublet; t, triplet; m, multiplet. FT-IR spectra were recorded on a Perkin-Elmer One FT-IR spectrometer. HRMS data was obtained with ESI (electrospray ionization) mode. Cyclic voltammetry was performed in a three-electrode cell equipped with a Pt-disk working electrode, a glassy carbon counter-electrode, and Ag/AgCl was used as the reference electrode. The electrochemical experiments were carried out under dry and oxygen-free atmosphere in CH_2Cl_2 with $Bu_4N(PF_6)$ (0.1 M) as a support electrolyte. Absorption spectra were recorded on a Perkin Elmer Lambda 900 UV/Vis/NIR spectrometer. Emission spectra were measured on a Perkin Elmer LS50B luminescence spectrometer. Melting point was measured with a Büchi B-540 microscope apparatus.

Materials

4,10-Dibromo-6,12-bis(octyloxy)anthanthrene (**1**),[8a] 4-(2-ethylhexyloxy)phenyl-4,4,5,5-tetramethyl-1,3,2-dioxaborolane[15] and 2-[4-[bis(4-methylphenyl)amino]phenyl]-4,4,5,5-tetramethyl-1,3,2-dioxaborolane (**3**)[16] were prepared according to literature procedures. 4,10-Dibromoanthanthrone was a courtesy from Heubach GmbH as Monolite Red 316801 product. All reactions were carried out under nitrogen or argon. Unless stated otherwise, all other reagents were purchased from commercial sources and used without additional purification.

Synthesis of 4,10-Bis(5-formyl-2-thienyl)-6,12-bis(octyloxy)anthanthrene (2). Compound **1** (50 mg, 0.072 mmol), 5-formylthiophene-2-boronic acid (45 mg, 0.2[illegible]0 mmol), Pd(dppf)Cl_2 (12 mg, 0.0144 mmol) and K_2CO_3 (0.1 g, 0.72 mmol) were mixed in dry toluene (6 mL) and dry methanol (6 mL) under argon. The reaction was carried out under microwave conditions (70 °C for 20 minutes). The mixture was filtered over silica gel, washed with CH_2Cl_2. The combined organic phases were evaporated and purified by column chromatography on silica gel using CH_2Cl_2:hexane = 1:1 (v/v) as eluent to give **2** as an orange solid. Yield: 25 mg (46%); m.p. 176-178 °C; IR (KBr): $\tilde{\nu}$ = 2922, 2852, 1676, 1449, 1384, 1350, 1220, 1065, 947, 903, 802, 746 cm^{-1}; ^{1}H NMR (300 MHz, $CDCl_3$): δ = 10.07 (s, 2H), 8.86 (d, *J* = 7.7 Hz, 2H), 8.64 (s, 2H), 8.56 (d, *J* = 7.4 Hz, 2H), 8.19 (t, *J* = 8.6 Hz, 2H), 7.99 (d, *J* = 3.[illegible] Hz, 2H), 7.67 (d, *J* = 3.8 Hz, 2H), 4.41 (t, *J* = 6.6 Hz, 4H), 2.1[illegible] 2.04 (m, 4H), 1.78-1.71 (m, 4H), 1.49-1.20 (m, 16H), 0.88 ppm (t, 6H); ^{13}C NMR (75 MHz, CD_2Cl_2): δ = 183.5, 152.6, 151.[illegible] 144.2, 137.6, 137.3, 132.0, 130.8, 129.7, 127.2, 126.8, 125.7, 125.5, 123.6, 122.1, 121.8, 120.3, 77.7, 32.4, 31.3, 30.2, 29.9, 27.0, 23.3, 14.3 ppm; HRMS (ESI): *m/z* calcd for $C_{48}H_{48}O_4S_2$: 752.2994; found: 752.2989.

Synthesis of Dye-1. A mixture of **2** (60 mg, 0.08 mmol), cyanoacetic acid (0.13 g, 1.6 mmol), ammonium acetate (30 mg, 0.4 mmol) and glacial acetic acid (50 mL) was purged with argon for 15 min, and then stirred at 125 °C for 48 h. After cooling to room temperature, the mixture was poured into ice water and the resulting precipitate was filtered off and washed with water three times. The purple solid was dissolved in CH_2Cl_2 (3 mL). Afterwards, hexane (20 mL) was added to precipitate the product. A dark red solid was obtained after filtration and dried in air. Yield: 52 mg (82%); m.p. > 340 °C decomposed; IR (KBr): $\tilde{\nu}$ = 2920, 1675, 1631, 1558, 1420, 1252, 1180, cm^{-1}; ^{1}H NMR (300 MHz, [D_8] THF): δ = 10.83 (s, 2H), 8.90 (d, *J* = 8.0 Hz, 2H), 8.71 (s, 2H), 8.63 (d, *J* = 7.4 Hz, 2H), 8.54 (s, 2H), 8.22 (t, *J* = 8.0 Hz, 2H), 8.15 (d, *J* = 4.0 Hz, 2H), 7.79 (d, *J* = 4.0 Hz, 2H), 4.46 (t, *J* = 6.4 Hz, 4H), 2.21-2.16 (m, 4H), 1.89-1.80 (m, 4H), 1.54-1.35 (m, 16H), 0.91 ppm (t, 6H); ^{13}C NMR (75 MHz, [D_8] THF): δ = 164.1, 152.5, 151.9, 146.8, 139.0, 137.5, 132.4, 131.3, 130.4, 127.3, 126.1, 124.2, 122.3, 120.7, 118.6, 116.7, 101.2, 77.9, 33.1, 31.9, 30.8, 30.5, 27.5, 23.8, 14.6 ppm; HRMS (ESI): *m/z* calcd for $C_{54}H_{50}N_2O_6S_2$: 886.3110; found: 886.3112.

Synthesis of 4-Bromo-10-[4-[bis(4-methylphenyl)amino]phenyl]-6,12-bis(octyloxy)anthanthrene (4). A mixture of **1** (1.38 g, 2 mmol), **3** (0.8 mg, 2 mmol), tetrakis(triphenylphosphine)-palladium(0) (117 mg, 0.1 mmol), toluene (400 mL), ^{t}BuOH (80 mL) and aqueous sodium carbonate (2 M, 80 mL) was placed in a round-bottomed flask under vacuum and then backfilled with N_2 three times before refluxing at 105 ºC for 20 h. After cooling to room temperature, the layers were separated. The aqueous phase was extracted with ethyl acetate (3 × 100 mL) and the combined organic phase was washed with brine (2 × 200 mL), dried over $MgSO_4$, filtered, and the solvent was removed. The

residue was purified by column chromatography over silica gel using CH_2Cl_2:hexane = 1:1 (v/v) as eluent to afford **4** as a yellow solid. Yield: 860 mg (49%); m.p. 155-157 °C; IR (KBr): $\tilde{\nu}$ = 2922, 2852, 1606, 1506, 1320, 1270, 1173, 813, 744 cm^{-1}; ^1H NMR (300 MHz, $CDCl_3$): δ = 8.93-8.78 (m, 3H), 8.66 (d, *J* = 7.5 Hz, 1H), 8.42-8.44 (m, 2H), 8.25 (t, *J* = 7.9 Hz, 1H), 8.25 (t, *J* = 7.9 Hz, 2H), 7.62 (d, *J* = 8.6 Hz, 2H), 7.33-7.19 (m, 10H), 4.51–4.29 (m, 4H), 2.39 (s, 6H), 2.29-2.08 (m, 4H), 1.73-1.80 (m, 4H), 1.61-1.20 (m, 16H), 0.94 ppm (m, 6H); ^{13}C NMR (75 MHz, $CDCl_3$): δ = 149.5, 149.4, 148.1, 145.5, 140.1, 133.8, 133.0, 131.7, 130.9, 130.6, 130.2, 126.4, 126.3, 126.1, 126.0, 125.2, 124.9, 124.7, 124.5, 124.0, 123.6, 122.4, 122.2, 122.1, 121.9, 121.0, 120.1, 119.3, 32.1, 32.0, 30.9, 29.9, 29.8, 29.5, 26.5, 22.9, 21.0, 14.3 ppm; HRMS (ESI): *m/z* calcd for $C_{58}H_{60}BrNO_2$: 881.3807; found: 881.3788.

Synthesis of 4-(5-Formyl-2-thienyl)-10-[4-[bis(4-methylphenyl)amino]phenyl]-6,12-bis(octyloxy)anthanthrene (5). Compound **4** (88 mg, 0.1 mmol), 5-carboxythiophene-2-boronic acid (31 mg, 0.2 mmol), $Pd(dppf)Cl_2$ (16 mg, 0.02 mmol) and K_2CO_3 (138 mg, 1 mmol) were mixed in dry toluene (6 mL) and dry methanol (6 mL) under argon. The reaction was carried out under microwave conditions (70 °C for 1 hour). The mixture was filtered over silica gel and washed with CH_2Cl_2. The combined organic phase was evaporated and purified by column chromatography on silica gel using CH_2Cl_2:hexane = 2:1 (v/v) as eluent to give **5** as an orange solid. Yield: 70 mg (77%); m.p. 178-180 °C; IR (KBr): $\tilde{\nu}$ = 2922, 2852, 1634, 1505, 1450, 1384, 1319, 1129, 815, 616 cm^{-1}; ^1H NMR (300 MHz, [D_6] DMSO): δ = 10.10 (s, 1H), 8.89–8.76 (m, 2H), 8.60 (s, 1H), 8.52 (d, *J* = 7.7 Hz, 1H), 8.34 (d, *J* = 7.9 Hz, 2H), 8.31-8.20 (m, 3H), 7.83 (s, 1H), 7.62 (d, *J* = 6.7 Hz, 2H), 7.21 (d, *J* = 7.8 Hz, 4H), 7.15 (d, *J* = 6.7 Hz, 2H), 7.11 (d, *J* = 7.8 Hz, 4H), 4.43 (d, *J* = 6.8 Hz, 4H), 2.39 (s, 6H), 2.09 (m, 4H), 1.71 (m, 4H), 1.39 (m, 16H), 0.86 ppm (d, 6H); ^{13}C NMR (75 MHz, CD_2Cl_2): δ = 183.0, 153.0, 150.7, 149.7, 148.1, 145.5, 143.5, 140.1, 136.8, 133.8, 133.1, 131.8, 131.2, 130.9, 130.3, 130.2, 129.0, 126.3, 126.2, 126.1, 126.0, 125.3, 125.2, 124.5, 124.1, 122.5, 122.3, 122.1, 121.5, 121.2, 120.9, 120.0, 119.9, 32.0, 31.0, 29.8, 29.5, 26.6, 26.5, 22.8, 21.0, 14.3 ppm; HRMS (ESI): *m/z* calcd for $C_{63}H_{63}NO_3S$: 913.4529; found: 913.4513.

Synthesis of Dye-2. A mixture of **5** (46 mg, 0.05 mmol), cyanoacetic acid (43 mg, 0.5 mmol), ammonium acetate (15 mg, 0.2 mmol) and glacial acetic acid (40 mL) was purged with argon for 15 min, and then stirred at 125 °C for 24 h. After cooling to room temperature, the mixture was poured into ice water and the resulting precipitate was filtered off, washed with water three times. The purple solid was dissolved in CH_2Cl_2 (3 mL). Afterwards, hexane (20 mL) was added to precipitate the product. The dark red solid was obtained by filtration and dried in air. Yield: 40 mg (71%); m.p. 218-220 °C; IR (KBr): $\tilde{\nu}$ = 2921, 2852, 1710, 1631, 1506, 1464, 1269, 1180 cm^{-1}; ^1H NMR (300 MHz, [D_8] THF): δ = 8.86 (t, *J* = 8.8 Hz, 2H), 8.72 (s, 1H), 8.59 (d, *J* = 7.5 Hz, 1H), 8.54 (s, 1H), 8.45 (s, 1H), 8.40 (d, *J* = 7.5 Hz, 1H), 8.25-8.10 (m, 3H), 7.78 (d, *J* = 3.9 Hz, 1H), 7.62 (d, *J* = 8.6 Hz, 2H), 7.22 (d, *J* = 8.6 Hz, 2H), 7.18-7.07 (m, 8H), 4.48-4.41 (m, 4H), 2.33 (s, 6H), 2.21-2.13 (m, 4H), 1.87-1.77 (m, 4H), 1.61-1.19 (m, 16H), 0.93-0.89 ppm (m, 6H); ^{13}C NMR (75 MHz, [D_8] THF): δ = 164.1, 152.8, 151.8, 150.8, 149.3, 146.8, 146.6, 141.1, 139.0, 137.4, 134.8, 133.8, 132.3, 131.6, 131.3, 131.0, 130.3, 127.3, 127.2, 127.0, 126.1, 123.3, 122.9, 122.1, 101.1, 77.8, 77.3, 33.1, 33.0, 31.9, 31.8, 30.8, 30.53, 30.50, 27.6, 27.5, 23.8, 23.7, 21.1, 14.6 ppm; HRMS (ESI): *m/z* calcd for $C_{66}H_{64}N_2O_4S$: 980.4587; found: 980.4582.

Synthesis of 4,10-Bis[4-(2-ethylhexyl)phenyl]anthanthrone (6). A mixture of 4,10-dibromoanthanthrone (1.85g, 4 mmol), 4-(2-ethylhexyloxy)phenyl-4,4,5,5-tetramethyl-1,3,2-dioxaborolane (3.32 g, 10 mmol), $Pd(PPh_3)_4$ (0.02 g, 0.017 mmol), 18-crown-6 (0.02 g, 0.076 mmol), toluene (250 mL), EtOH (25 mL) and aqueous potassium carbonate (2 M, 40 mL) was placed in a round-bottomed flask under vacuum and then backfilled with N_2 three times before refluxing at 105 ºC for 20 h. After cooling to room temperature, the layers were separated. The aqueous phase was extracted with CH_2Cl_2 (3 × 100 mL), and the combined organic phase was washed with brine (2 × 200 mL), dried over $MgSO_4$, filtered, and the solvent was removed. The residue was purified by column chromatography over silica gel using CH_2Cl_2:hexane = 2:1 (v/v) as eluent to afford **6** as a red solid. Yield: 2.0 g (70%); m.p. 313-315 °C; IR (KBr): $\tilde{\nu}$ = 2924, 1652, 1606, 1581, 1503, 1467, 1382, 1272, 1241, 1175, 1032, 940, 838, 765, 597 cm^{-1}; ^1H NMR (300 MHz, CD_2Cl_2): δ = 8.52 (d, *J* = 7.2 Hz, 2H), 8.32 (d, *J* = 8.3 Hz, 2H), 8.24 (s, 2H), 7.72 (t, *J* = 7.8 Hz, 2H), 7.52 (d, *J* = 8.6 Hz, 4H), 7.12 (d, *J* = 8.6 Hz, 4H), 4.00 (d, *J* = 5.8 Hz, 4H), 1.85-1.79 (m, 2H), 1.63-1.26 (m, 16H), 1.03-0.93 ppm (m, 12H); ^{13}C NMR (75 MHz, CD_2Cl_2): δ = 160.2, 143.2, 134.4, 133.4, 132.1, 131.7, 130.7, 129.6, 127.0, 126.9, 125.0, 115.1, 71.3, 40.1, 31.1, 29.7, 24.5, 23.7, 14.5, 11.5 ppm; HRMS (ESI): *m/z* calcd for $C_{50}H_{51}O_4$: 715.3782; found: 715.3781($M+H^+$).

Synthesis of 4,10-Bis[4-(2-ethylhexyl)phenyl]anthanthrene (7). Under N_2 protection, **6** (2 g, 2.8 mmol) was dissolved in dry THF (300 mL). BH_3·THF (1 M, 10 mL, 10 mmol) was slowly added to the above suspension while stirring. The reaction mixture was stirred at 70 °C under nitrogen for 3 h. The solution was cooled and the excess of BH_3·THF was quenched with methanol. The mixture was filtered off and the solvent evaporated in vacuo to produce a yellowish solid. The crude product was purified by column chromatography on silica gel using CH_2Cl_2:hexane = 1:4 (v/v) as eluent to afford **7** as a light yellow solid. Yield: 0.4 g (21%); m.p. 223-224 °C; IR (KBr): $\tilde{\nu}$ = 2954, 2925, 2859, 1606, 1507, 1460, 1383, 1282, 1244, 1172, 1033, 891, 828, 762, 693 cm^{-1}; ^1H NMR (300 MHz, $CDCl_3$): δ = 8.85 (s, 2H), 8.56 (d, *J* = 7.8 Hz, 2H), 8.29 (d, *J* = 7.4 Hz, 2H), 8.12 (s, 2H), 8.10 (t, *J* = 7.8 Hz, 2H), 7.70 (d, *J* = 8.6 Hz, 4H), 7.15 (d, *J* = 8.6 Hz, 4H), 4.00 (d, *J* = 5.8 Hz, 4H), 1.86-1.80 (m, 2H), 1.61-1.38 (m, 16H), 1.04-0.94 ppm (m, 12H); ^{13}C NMR (75 MHz, CD_2Cl_2): δ = 159.9, 140.9, 132.0, 131.7, 131.4, 131.1, 128.8, 126.7, 126.4, 125.0, 123.8, 115.2, 115.0, 71.4, 40.2, 31.2, 29.8, 24.6, 23.7, 14.5, 11.6 ppm; HRMS (ESI): *m/z* calcd for $C_{50}H_{52}O_2$: 684.3967; found: 684.3970.

Synthesis of 4,10-Bis[4-(2-ethylhexyl)phenyl]-6,12-dibromoanthanthrene (8). Compound **7** (220 mg, 0.32 mmol) was dissolved in CH_2Cl_2 (50 mL). Br_2 (102 mg in 5 mL CH_2Cl_2, 0.64 mL) was added dropwise. The reaction mixture was stirred for 1 h. After the removal of CH_2Cl_2, the residue was

washed by hexane (20 mL) to afford **8** as a green-yellow solid. Yield: 230 mg (86%); m.p. 263-265 °C; IR (KBr): $\tilde{\nu}$ = 2958, 2921, 2855, 1606, 1577, 1506, 1464, 1431, 1350, 1283, 1243, 1171, 1026, 997, 920, 831, 758, 645 cm^{-1}; ^1H NMR (300 MHz, $CDCl_3$): δ = 9.14 (d, *J* = 8.3 Hz, 2H), 8.69 (s, 1H), 8.39 (d, *J* = 7.5 Hz, 2H), 8.19 (d, *J* = 8.0 Hz, 2H), 7.70 (d, *J* = 8.6 Hz, 2H), 7.17 (d, *J* = 8.6 Hz, 2H), 4.01 (d, *J* = 5.7 Hz, 4H), 1.87-1.83 (m, 2H), 1.62-1.38 (m, 16H), 1.04-0.96 ppm (m, 12H); ^{13}C NMR (75 MHz, $CDCl_3$): δ = 162.4, 160.0, 142.1, 132.6, 131.4, 131.3, 130.1, 129.4, 128.0, 127.2, 127.1, 125.1, 122.7, 114.8, 70.9, 39.7, 30.8, 29.3, 24.2, 23.3, 14.3, 11.4 ppm; HRMS (ESI): *m/z* calcd for $C_{50}H_{50}Br_2O_2$: 840.2172; found: 840.2161.

Synthesis of 4,10-Bis[4-(2-ethylhexyl)phenyl]-6,12-bis(5-formyl-2-thienyl)anthanthrene (9). Compound **8** (126 mg, 0.15 mmol), 5-formylthiophene-2-boronic acid (93 mg, 0.6 mmol), $Pd(dppf)Cl_2$ (25 mg, 0.03 mmol) and K_2CO_3 (0.1 g, 0.72 mmol) were mixed in toluene (6 mL) and dry methanol (6 mL) under argon. The reaction was carried out under microwave conditions (70 °C for 1 h). The mixture was filtered over silica gel and washed with CH_2Cl_2. The combined organic phase was evaporated and purified by column chromatography on silica gel using CH_2Cl_2:pentane = 4:1 (v/v) as eluent to give **9** as an orange solid. Yield: 120 mg (88%); m.p. 311-313 °C; IR (KBr): $\tilde{\nu}$ = 2956, 2923, 2857, 1667, 1606, 1507, 1452, 1383, 1246, 1221, 1043, 837, 765, 662 cm^{-1}; ^1H NMR (300 MHz, CD_2Cl_2): δ = 10.09 (s, 2H), 8.35 (m, 4H), 8.06-8.11 (m, 4H), 7.96 (s, 2H), 7.54-7.59 (m, 6H), 7.09 (d, *J* = 8.6 Hz, 2H), 3.96 (d, *J* = 5.7 Hz, 4H), 1.82-1.77 (m, 2H), 1.60-1.26 (m, 16H), 1.00-0.91 ppm (m, 12H); ^{13}C NMR (75 MHz, CD_2Cl_2): δ = 183.5, 160.0, 150.2, 146.0, 141.9, 137.6, 131.4, 130.4, 127.0, 126.3, 125.8, 125.1, 123.2, 122.7, 115.1, 71.2, 40.0, 31.1, 29.7, 24.5, 23.7, 14.5, 11.5 ppm; HRMS (ESI): *m/z* calcd for $C_{60}H_{56}O_4S_2$: 904.3615; found: 904.3627.

Synthesis of Dye-3. A mixture of **9** (45 mg, 0.05 mmol), cyanoacetic acid (85 mg, 1.0 mmol), ammonium acetate (19 mg, 0.25 mmol) and glacial acetic acid (40 mL) was purged with argon for 15 min, and then stirred at 125 °C for 24 h. After cooling to room temperature, the mixture was poured into ice water and the resulting precipitate was filtered off and washed with water 3 times. The purple solid was dissolved in CH_2Cl_2 (3mL). Afterwards, hexane (20 mL) was added to precipitate the product. A dark red solid was obtained after filtration and dried in air. Yield: 40 mg (77%); m.p. 261-263 °C; IR (KBr): $\tilde{\nu}$ = 2923, 2219, 1693, 1581, 1506, 1412, 1360, 1243, 1203, 1175, 1030, 833, 764, 655, 588 cm^{-1}; ^1H NMR (300 MHz, [D_8] THF): δ = 8.57 (s, 2H), 8.42 (d, *J* = 8.2 Hz, 2H), 8.37 (d, *J* = 7.4 Hz, 4H), 8.24 (d, *J* = 3.8 Hz, 2H), 8.12 (t, *J* = 7.9 Hz, 2H), 8.01 (s, 2H), 7.64 (d, *J* = 3.7 Hz, 2H), 7.58 (d, *J* = 8.5 Hz, 4H), 7.11 (d, *J* = 8.6 Hz, 4H), 3.99 (d, *J* = 5.5 Hz, 4H), 1.85-1.75 (m, 2H), 1.66-1.25 (m, 16H), 1.06-0.89 ppm (m, 12H); ^{13}C NMR (75 MHz, [D_8] THF): δ = 164.1, 160.6, 150.1, 146.8, 142.7, 139.4, 139.1, 133.6, 133.1, 132.1, 132.0, 131.0, 127.6, 126.6, 125.7, 116.7, 115.6, 101.5, 71.2, 40.8, 31.8, 30.2, 24.4, 14.6, 11.7 ppm; HRMS (ESI): *m/z* calcd for $C_{66}H_{58}N_2O_6S_2$: 1038.3736; found: 1038.3730.

Synthesis of 4,10-[4-(2-Ethylhexyl)phenyl]-6-bromo-12-[4-[bis(4-methylphenyl)amino]phenyl]anthanthrene (10). A mixture of **8** (210 mg, 0.25 mmol), **3** (100 mg, 0.25 mmol), tetrakis(triphenylphosphine)-palladium(0) (14.4 mg, 0.0125 mmol), toluene (50 mL), ^{t}BuOH (10 mL) and aqueous sodium carbonate (2 M, 10 mL) was placed in a round-bottomed flask under vacuum and then backfilled with N_2 for three times before refluxing at 105 ºC for 16 h. After cooling to room temperature, the layers were separated. The aqueous phase was extracted with ethyl acetate (3 × 50 mL), and the combined organic phases were washed with brine (2 × 50 mL), dried over $MgSO_4$, filtered off, and the solvent was removed. The residue was purified by column chromatography on silica gel using CH_2Cl_2:hexane = 1:3 (v/v) as eluent to afford **10** as a yellow solid. Yield: 136 mg (53%); m.p. 102-103 °C; IR (KBr): $\tilde{\nu}$ = 2921, 2854, 1605, 1507, 1467, 1383, 1318, 1281, 1242, 1174, 1107, 1032, 832, 761, 574 cm^{-1}; ^1H NMR (300 MHz, [D_6] DMSO): δ = 9.08 (d, *J* = 7.8 Hz, 1H), 8.59 (s, 1H), 8.39-8.29 (m, 4H), 8.19 (t, *J* = 7.9 Hz, 2H), 7.86 (s, 2H), 7.72 (d, J = 8.5 Hz, 2H), 7.56 (d, *J* = 8.5 Hz, 2H), 7.49 (d, *J* = 8.4 Hz, 2H), 7.25 (d, *J* = 8.5 Hz, 2H), 7.21-7.16 (m, 8H), 7.12 (d, J = 8.4 Hz, 4H), 4.05 (m, 4H), 2.32 (s, 6H), 1.82 (m, 2H), 1.64-1.21 (m, 16H), 1.07-0.9[illegible] ppm (m, 12H); ^{13}C NMR (75 MHz, $CDCl_3$): δ = 159.5, 159.3, 148.0, 145.4, 133.3, 133.1, 130.0, 132.4, 131.5, 131.4, 131.2, 131.1, 130.3, 130.2, 125.4, 121.7, 121.6, 114.8, 114.6, 70.9, 70.8, 39.7, 30.8, 29.3, 24.2, 23.3, 21.0, 14.3, 11.4 ppm; HRMS (ESI): *m/z* calcd for $C_{70}H_{68}BrNO_2$: 1033.4428; found: 1033.4442.

Synthesis of 4,10-[4-(2-Ethylhexyl)phenyl]-6-(5-formyl-2-thienyl)-12-[4-[bis(4-methylphenyl)amino]phenyl] anthanthrene (11). Compound **10** (156 mg, 0.15 mmol), 5-formylthiophene-2-boronic acid (47 mg, 0.3 mmol), $Pd(dppf)Cl_2$ (12 mg, 0.015 mmol) and K_2CO_3 (210 mg, 1.5 mmol) were mixed in dry toluene (7 mL) and dry methanol (7 mL) under argon. The reaction was carried out under microwave conditions (70 °C for 1 hour). The mixture was filtered over silica gel and washed with CH_2Cl_2. The combined organic phase was evaporated and purified by column chromatography on silica gel using CH_2Cl_2:hexane = 3:1 (v/v) as eluent to give **11** as an orange solid. Yield: 75 mg (47%); m.p. 197-198 °C; IR (KBr): $\tilde{\nu}$ = 2921, 1672, 1605, 1506, 1456, 1383, 1318, 1243, 1174, 1034, 813, 764, 573 cm^{-1}; ^1H NMR (300 MHz, CD_2Cl_2): δ = 10.11 (s, 1H), 8.43 (d, *J* = 8.3 Hz, 1H), 8.37-8.23 (m, 3H), 8.09-8.02 (m, 4H), 7.94 (s, 1H), 7.63 (d, *J* = 5.9 Hz, 2H), 7.60 (d, *J* = 5.9 Hz, 2H), 7.52 (d, *J* = 3.7 Hz, 1H), 7.47 (d, *J* = 8.4 Hz, 3H), 7.31-7.10 (m, 14H), 4.00 (m, 4H), 1.87-1.81 (m, 2H), 1.74-1.14 (m, 16H), 1.10-0.86 ppm (m, 12H); ^{13}C NMR (75 MHz, CD_2Cl_2): δ = 183.5, 159.9, 145.92 (s), 141.9, 137.6, 133.4, 132.83 (s), 131.7, 131.4, 130.6, 127.6, 126.2, 125.8, 124.9, 123.5, 122.1, 115.1, 71.3, 40.1, 31.2, 30.3, 29.8, 24.6, 23.7, 21.2, 14.5, 11.5; HRMS (ESI): *m/z* calcd for $C_{75}H_{71}NO_3S$ 1065.5155; found: 1065.5158.

Synthesis of Dye-4. A mixture of **11** (43 mg, 0.04 mmol), cyanoacetic acid (34 mg, 0.4 mmol), ammonium acetate (15 mg, 0.2 mmol) and glacial acetic acid (30 mL) was purged with argon for 15 min, and then stirred at 125 °C for 24 h. After cooling to room temperature, the mixture was poured into ice water and the resulting precipitate was filtered off, washed with water for three times. The purple solid was dissolved in CH_2Cl_2 (3 mL). Afterwards, hexane (20 mL) was added to precipitate the product. A dark red solid was obtained after filtration and was dried in air. Yield: 36 mg (79%); m.p. 131-13[illegible]

°C; IR (KBr): $\tilde{\nu}$ = 2923, 1606, 1507, 1445, 1243, 1175,1180, 813 cm^{-1}; ^1H NMR (300 MHz, [D_8] THF): δ = 8.58 (s, 1H), 8.43 (d, *J* = 8.1 Hz, 1H), 8.36-8.29 (m, 3H), 8.24 (d, *J* = 3.8 Hz, 1H), 8.09 (d, *J* = 2.4 Hz, 1H), 8.06 (d, *J* = 2.4 Hz, 1H), 8.04 (s, 1H), 7.98 (s, 1H), 7.62-7.57 (m, 5H), 7.49 (d, *J* = 8.5 Hz, 2H), 7.27 (d, *J* = 8.6 Hz, 2H), 7.20-7.06 (m, 11H), 4.01 (m, 4H), 2.33 (s, 6H), 1.86-1.75 (m, 2H), 1.75-1.24 (m, 16H), 1.07-0.91 ppm (m, 12H); ^{13}C NMR (75 MHz, $CDCl_3$): δ = 164.1, 160.5, 150.8, 149.2, 146.4, 139.3, 138.3, 134.0, 133.9, 133.3, 132.9, 132.2, 132.0, 129.3, 127.3, 126.8, 126.3, 125.4, 122.2, 116.6, 116.0, 115.5, 101.2, 71.2, 40.8, 31.8, 30.3, 24.2, 21.1, 14.6, 11.7 ppm; HRMS (ESI): *m/z* calcd for $C_{78}H_{72}N_2O_4S$: 1132.5207; found: 1132.5211.

Fabrication of DSSCs

Electrodes with 8 µm transparent layer and 5 µm scattering layer of TiO_2 were screen-printed on fluorine-doped tin oxide (FTO) as reported in the literature.[17] After sintering at 500 °C for 0.5 h and cooling to room temperature, the electrodes were treated with 33 mM $TiCl_4$ solution at 70 °C for 0.5 h. The films were sintered at 500 °C for 0.5 h and cooled to 80 °C before dipping into the dye solution (0.1 mM dye in THF) for 12 h. After the sensitization, the electrodes were rinsed with acetonitrile and dried in air. The cells were sealed with a Surlyn film and a platinized FTO counter electrode. The electrolyte composition of this study was 1.0 M 1,3-dimethylimidazolium iodide, 0.05 M LiI, 0.03 M I_2, 0.1 M guanidiniumthiocyanate and 0.5 M 4-tert-butylpyridine in acetonitrile:valeronitrile (85:15, v/v). The area of the DSSC is 0.28 cm^{-2} while the DSSC was tested under a mask with an area of 0.16 cm^{-2}.

Computational modeling

Electronic structure and excitation calculations were performed with the Gaussian09 software package[18] using Pople's split-valence 6-31+G(d,p) basis set augmented with diffuse and polarization functions.[19] Geometry optimization of the isolated ground state molecule was carried out within the density functional theory (DFT) framework[20] using the M06[21] exchange–correlation functional, applying no symmetry constraints. The 10 lowest lying electronic excitations were calculated within the time-dependent DFT formalism[22] using the M06-2X[21] xc approximation. We ran an auxiliary set of calculations at the CAM-B3LYP/6-31+G(d,p)[23] level for **Dye-2** and **Dye-4** to cross-check the reliability of the chosen functional. These excitations are in good agreement with the results obtained from M06-2X (Tables S1-S4).

Acknowledgements

Financial support for this research by the Swiss National Science Foundation (Grant No. 200021-147143) is gratefully acknowledged. MC acknowledges the support of the Norwegian Research Council through the CoE Centre for Theoretical and Computational Chemistry (CTCC) Grant Nos. 179568/V30 and 171185/V30.

Notes and references

1 (a) K. N. Winzenberg, P. Kemppinen, G. Franchini, M. Bown, G. E. Collis, C. M. Forsyth, K. Hegedus, Th. B. Sing and S. E. Watkins, *Chem. Mater.*, 2009, **21**, 5701; (b) K. B. Burke, Y. Shu, P. Kemppinen, B. Singh, M. Bown, I. I. Liaw, R. M. Williamson, L. Thomsen, P. Dastoor, W. Belcher, C. Forsyth, K. N. Winzenberg and G. E. Collis, *Cryst. Growth Des.*, 2012, **12**, 725; (c) R. Gardia, G. Malloci, A. Mattoni and G. Cappellini, *J. Phys. Chem. A*, 2014, **118**, 5170.

2 (a) J.-B. Giguère, J. Boismenu-Lavoie and J.-F. Morin, *J. Org. Chem.*, 2014, **79**, 2404; (b) A. Malikal, K. Raghavachari, H. Katz, E. Chnadross and T. Siegrist, *Chem. Mater.*, 2004, **16**, 4980; (c) W. Fudickar and T. Linker, *J. Am. Chem. Soc.*, 2012, **134**, 15071.

3 B. K. Shah, D. C. Neckers, J. Shi, E. W. Forsythe and D. Morton, *J. Phys. Chem. A*, 2005, **109**, 7677.

4 S. K. Sugunan, C. Greenwald, M. F. Paige and R. P. Steer, *J. Phys. Chem. A*, 2013, **117**, 5419.

5 T. Matsuno, S. Kamata, S. Hitosugi and H. Isobe, *Chem. Sci.*, 2013, **4**, 3179.

6 L. Zhang, B. Walker, F. Liu, N. S. Colella, S. C. B. Mannsfeld, J. Watkins, T.-Q. Nguyen and A. L. Briseno, *J. Mater. Chem.*, 2012, **22**, 4266.

7 J.-B. Giguere, N. S. Sariciftci and J.-F. Morin, *J. Mater. Chem. C*, 2015, **3**, 601.

8 (a) J.-B. Giguère, Q. Verolet and J.-F. Morin, *Chem. Eur. J.*, 2013, **19**, 372; (b) J.-B. Giguère and J.-F. Morin, *J. Org. Chem.*, 2013, **78**, 12769.

9 (a) Y. Geng, S. Sangtarash, C. Huang, H. Sadeghi, Y. Fu, W. Hong, T. Wandlowski, S. Decurtins, C. J. Lambert and S.-X. Liu, *J. Am. Chem. Soc.*, 2015, **137**, 4469; (b) S. Sangtarash, C. Huang, H. Sadeghi, G. Sorohhov, J. Hauser, T. Wandlowski, W. Hong, S. Decurtins, S.-X. Liu and C. J. Lambert, *J. Am. Chem. Soc.*, 2015, **137**, 11425.

10 (a) Y. Geng, F. Pop, C. Yi, N. Avarvari, M. Grätzel, S. Decurtins and S.-X. Liu, *New J. Chem.*, 2014, **38**, 3269; (b) H. Li, C. Yi, S. Moussi, S.-X. Liu, C. Daul, M. Grätzel and S. Decurtins, *RSC Adv.*, 2013, **3**, 19798; (c) A. S. Hart, K. C. Chandra Bikram, N. K. Subbaiyan, P. A. Karr and F. D'Souza, *ACS Appl. Mat. Interfaces*, 2012, **4**, 5813.

11 (a) J. J. Bergkamp, S. Decurtins and S.-X. Liu, *Chem. Soc. Rev.*, 2015, **44**, 863; (b) J. Wu, N. Dupont, S.-X. Liu, A. Neels, A. Hauser and S. Decurtins, *Chem. Asian J.*, 2009, **4**, 392.

12 A. Amacher, C. Yi, J. Yang, M. P. Bircher, Y. Fu, M. Cascella, M. Grätzel, S. Decurtins and S.-X. Liu, *Chem. Commun.*, 2014, **50**, 6540.

13 (a) A. Mishra, M. K. R. Fischer and P. Bäuerle, *Angew. Chem. Int. Ed.*, 2009, **48**, 2474; (b) A. Hagfeldt, G. Boschloo, L. Sun, L. Kloo and H. Pettersson, *Chem. Rev.*, 2010, **110**, 6595; (c) J. N. Clifford, E. Martinez-Ferrero, A. Viterisi and E. Palomares, *Chem. Soc. Rev.*, 2011, **40**, 1635.

14 (a) J. A. Mikroyannidis, A. Kabanakis, P. Balraju and G. D. Sharma, *J. Phys. Chem. C*, 2010, **114**, 12355; (b) G. Zhang, H. Bala, Y. Cheng, D. Shi, X. Lv, Q. Yu and P. Wang, *Chem. Commun.*, 2009, 2198.

15 S.-C. Lo, E. B. Namdas, P. L. Burn and I. D. W. Samuel, *Macromolecules*, 2003, **36**, 9721.

16 H. Li, H. Luo, Z. Cao, Z. Gu, P. Shen, B. Zhao, H. Chen, G. Yu and S. Tan, *J. Mater. Chem.*, 2012, **22**, 22913.

17 H. N. Tsao, P. Comte, C. Y. Yi and M. Grätzel, *ChemPhysChem*, 2012, **13**, 2976.

18 M. J. Frisch, G. W. Trucks, H. B. Schlegel, G. E. Scuseria, M. A. Robb, J. R. Cheeseman, G. Scalmani, V. Barone, B. Mennucci, G. A. Petersson, H. Nakatsuji, M. Caricato, X. Li, H. P. Hratchian, A. F. Izmaylov, J. Bloino, G. Zheng, J. L. Sonnenberg, M. Hada, M. Ehara, K. Toyota, R. Fukuda, J. Hasegawa, M. Ishida, T. Nakajima, Y. Honda, O. Kitao, …

Nakai, T. Vreven, J. A. Montgomery, Jr, J. E. Peralta, F. Ogliaro, M. Bearpark, J. J. Heyd, E. Brothers, K. N. Kudin, V. N. Staroverov, R. Kobayashi, J. Normand, K. Raghavachari, A. Rendell, J. C. Burant, S. S. Iyengar, J. Tomasi, M. Cossi, N. Rega, J. M. Millam, M. Klene, J. E. Knox, J. B. Cross, V. Bakken, C. Adamo, J. Jaramillo, R. Gomperts, R. E. Stratmann, O. Yazyev, A. J. Austin, R. Cammi, C. Pomelli, J. W. Ochterski, R. L. Martin, K. Morokuma, V. G. Zakrzewski, G. A. Voth, P. Salvador, J. J. Dannenberg, S. Dapprich, A. D. Daniels, O. Farkas, J. B. Foresman, J. V. Ortiz, J. Cioslowski and D. J. Fox, Gaussian 09, Revision A.02, Gaussian, Inc., Wallingford, CT, 2009.

19 (a) R. Ditchfield, W. J. Hehre and J. A. Pople, *J. Chem. Phys.*, 1971, **54**, 724; (b) T. Clark, J. Chandrasekhar, G. W. Spitznagel and P. v. R. Schleyer, *J. Comp. Chem.*, 1983, **4**, 294; (c) M. J. Frisch, J. A. Pople and J. S. Binkley, *J. Chem. Phys.*, 1984, **80**, 3265.

20 (a) P. Hohenberg and W. Kohn, *Phys. Rev. B*, 1964, **136**, 864; (b) W. Kohn and L. J. Sham, *Phys. Rev. A*, 1965, **140**, 1133.

21 Y. Zhao and D. G. Truhlar, *Theor. Chem. Acc.*, 2006, **120**, 215.

22 E. Runge and E. K. U. Gross, *Phys. Rev. Lett.*, 1984, **52**, 996.

23 (a) A. D. Becke, *J. Chem. Phys.*, 1993, **98**, 5648; (b) C. Lee, W. Yan, R. G. Parr, *Phys. Rev. B*, 1988, **37**, 785; (c) S. H. Vosko, L. Wilk and M. Nusair, *Can. J. Phys.*, 1980, **58**, 1200; (d) P. J. Stephens, F. J. Devlin, C. F. Chabalowski and M. J. Frisch, *J. Phys. Chem.*, 1994, **98**, 11623; (e) T. Yanai, D. P. Tew and N. C. Handy, *Chem. Phys. Lett.*, 2004, **393**, 51.

Table of contents

Four anthanthrene-based molecules were synthesized as sensitizers in dye-sensitized solar cells, leading to the best overall efficiency up to 5.3%.